Summer 2018

Sequence Effects on the Glass Transition Temperature

William Drayer
wfd7@zips.uakron.edu

Sequence Effects on the Glass Transition Temperature

William Drayer

University of Akron

302 E Buchtel Ave

Akron, OH 44325-0001

Advisor: Dr. David S. Simmons

Sequence Effects on the Glass Transition Temperature

Background and Motivation

Lithium ion batteries (LIBs) are the industry standard for portable energy storage in small electronics. However, current LIBs scale poorly for use in larger devices; primarily, the organic electrolyte solvent in modern LIBs displays a narrow electrochemical stability window, low thermal stability, and flammability. These factors cause larger LIBs with these materials to be less resistant to thermal and mechanical abuse, rendering them unsafe and ineffective. Extensive literature exists on modifying these organic electrolyte solvents to improve their resistance to degradation, as well as lithium salts in these electrolyte solutions, such as lithium hexafluorophosphate, to increase ionic conductivity for larger energy requirements[1]. Still, commercial LIBs have exhibited catastrophic failure in the combustion of phone and electric vehicle battery fires.

To forgo use of organic carbonates altogether, alternative approaches to LIB technology include room temperature molten salts (or ionic liquids), ceramics, and polymers, all of which substantially change the structure of the electrolyte. Polymer electrolytes exhibit limited volatility and avoid cell leakage from mechanical abuse, with the latter leading to the possibility of flexible LIB design[1,2]. Specifically, polyethylene oxide (PEO) shows promise as a polyelectrolyte, as it has been shown to coordinate lithium ions and allow for their transfer along the polymer chain[3,4]. Here, we propose copolymerization of PEO and similar conductive backbone monomers with a monomer with vastly different dynamic characteristics, such as polystyrene (PS), to suppress T_g to improve chain mobility and therefore charge mobility while preserving the ion transfer properties exhibited in PEO to provide candidates for further study in LIB materials research. We expect the unfavorable interaction of these sample monomers due to the nonpolar, bulky phenyl group in PS monomers interfering with the polar crystalline structure of PEO.

Due to weak cross-interactions between the monomer species, highly alternating copolymers of PEO derivatives and PS monomers are expected to suppress the glass transition temperature beyond that anticipated by simple mixing rules, such as the Fox equation[5],

$$\frac{1}{T_g} = \frac{w_1}{T_{g,1}} + \frac{w_2}{T_{g,2}},$$

where T_g is the glass transition of the bulk copolymer, and w_i and $T_{g,i}$ are the weight fractions and glass transition temperatures of the pure i polymer, respectively. This behavior of reduced T_g in our system is expected to contrast the T_g enhancement seen in Tonelli, Jhon, and Genzer[6], as their work shows an increase in T_g due to favorable interactions. Furthermore, PS monomers distributed along an electrolyte chain may avoid crystallization at lower molecular weights, which causes higher ionic conductivity due to increased segmental motion in the polymer[7]. Upon successful completion of our proposed work, we hope to identify sequenced copolymer electrolytes for laboratory testing to development safer, effective lithium ion batteries.

Methodology

This work will consist of molecular dynamics simulations of the bulk copolymer, with the goal of identifying chains that exhibit a reduced T_g relative to the homopolymers while avoiding phase separation. We work with a coarse-grained Kremer and Grest model[8]. Cross-interaction energies will be reduced from an arbitrarily chosen reference value of unity to model the expected behavior of dissimilar monomers having unfavorable interactions. The effect of chain sequence and mean block length will be focused, to show that highly alternating patterns causes a frustration in the local structure by forcing unfavorable interactions, lowering T_g and preventing phase separation due to chain geometry.

Each polymer sequence will be subjected to the "PreSQ routine," consisting primarily of generation, quench, and equilibration steps, as shown in Figure 1. Once an initial high temperature polymer sample is equilibrated, the sample is quenched and configurations are saved at different temperatures determined by the algorithm. This allows relaxation times to be determined independently for multiple temperatures in decreasing order. The temperature-relaxation time pairs for each sample returned by this routine may then be fitted to a functional form such as Vogel-Fulcher-Tammann equation, or VFT[9–11], to compute a computational T_g, or T_g^{comp}. These T_g^{comp}s may then be correlated to the mean block size of the polymer chain, providing evidence that highly alternating copolymers with substantial amounts of unfavorable cross-interactions may exhibit suppressed T_g^{comp}s. Furthermore, equilibrated samples may be visualized using Visual Molecular Dynamics (VMD)[12] to qualitatively assess their degree of phase separation at the molecular level, as phase separation is to be avoided. Phase separation of the polymer would result in aggregations of non-electrolytic monomers which would interfere with uniform ionic conductivity; furthermore, phase separation would also be expected to interfere with the PEO-lithium transfer mechanism by reducing the number of sites that complexed lithium ions can be transferred through the system.
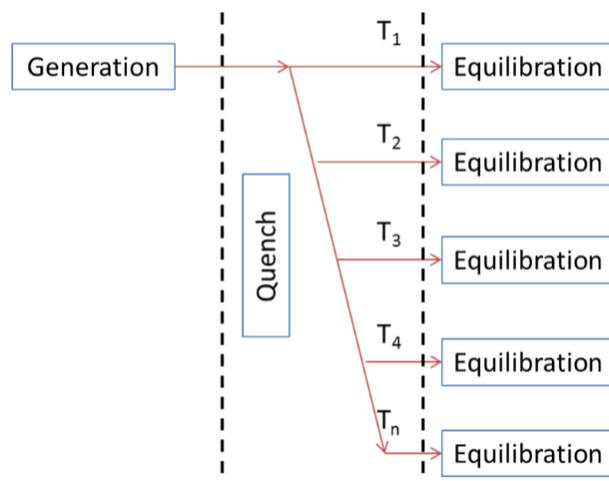
Figure 1. Reduced schematic for the PreSQ routine. This routine allows for independent equilibrations to expedite the determination of T_g^{comp}.

Simulations and Data

     All simulation work presented utilized LAMMPS[13] with the Kremer-Grest bead-spring model[8] consisting of two bead (monomer) types, denoted by A and B for an electrolyte and non-electrolyte, respectively. The dimensionless interaction energy between two nonbonded similar beads, ε_{AA} and ε_{BB}, is set to unity, while the cross-interaction, ε_{AB}, is some value less than unity, to emulate monomers that reduce the system energy by interacting with monomers of the same type. These pair interactions are described by the 12-6 Lennard-Jones (LJ) potential:

$$E_{LJ}^{ij} = 4\varepsilon_{ij}\left[\left(\frac{\sigma}{r}\right)^{12} - \left(\frac{\sigma}{r}\right)^{6}\right]$$

where σ is the range of the interaction, the dimensionless length of unity for both bead types, and r is the distance between beads i and j, in terms of σ. Bonded beads interact via the finitely extensible nonlinear elastic (FENE) potential[14]:

$$E_{bond}^{ij} = -\frac{KR_0^2}{2}\ln\left[1 - \left(\frac{r}{R_0}\right)^{2}\right] + 4\varepsilon_{ij}\left[\left(\frac{\sigma}{r}\right)^{12} - \left(\frac{\sigma}{r}\right)^{6}\right] + \varepsilon_{ij}$$

with standard constants $K = \frac{30\varepsilon}{\sigma^2}$ and $R_0 = 1.5\sigma$. The LJ potential and middle term of the FENE potential are truncated at a length of 2.5σ.
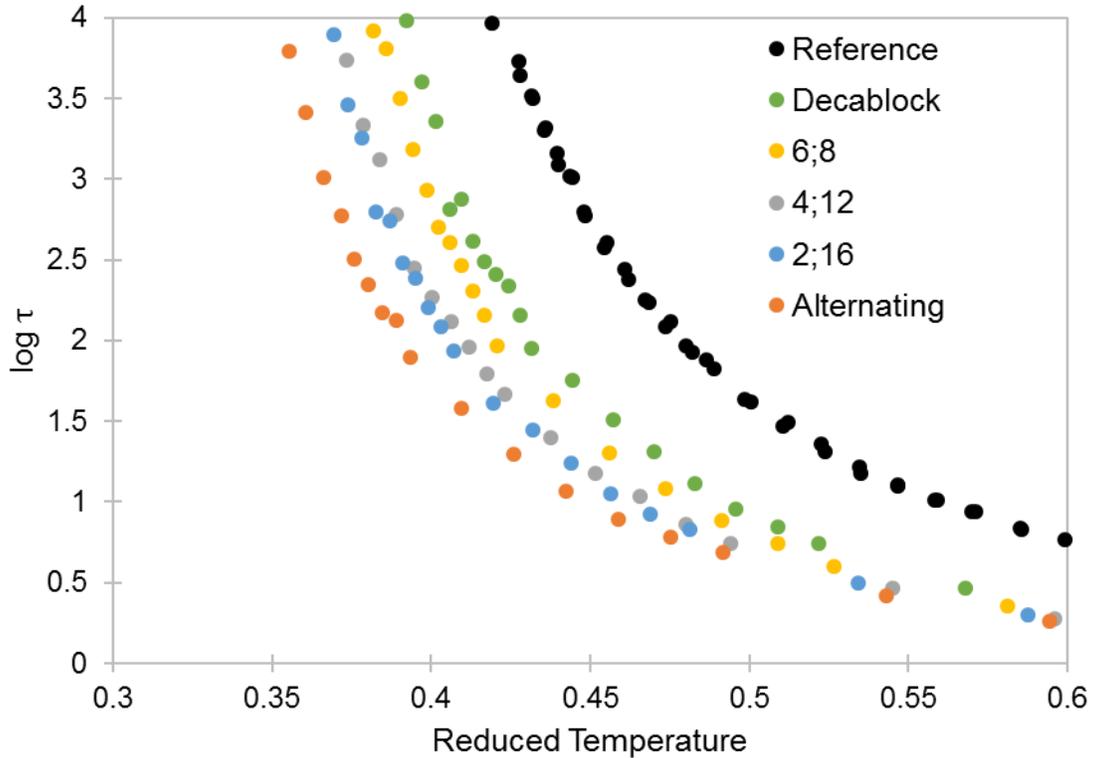
Figure 2. Relaxation curves for select chains. Reference is that of a pure homopolymer. Lines are guides-to-the-eye. For chain sequences between alternating and decablock chains, $i;j$ refers to a polymer with i blocks of length two and j blocks of length one.

All initial polymer configurations were generated using the PACKMOL software package[15]. Each sample consists of 400 identical polymer chains of a specific 20-mer sequence, subjected to periodic boundary conditions to produce the polymer behavior in bulk. The polymer sample is then brought to some high-temperature state in the first step of the PreSQ routine. The sample is then quenched while held at constant pressure, with polymer configurations being saved at evenly spaced temperature intervals. Each of these configurations is independently equilibrated at their saved temperature to determine the relaxation time, determined using the self-part of the intermediate scattering function[16] with a cutoff value of 0.2. These times are reported in the dimensionless LJ time unit, τ, with 1τ being on the order of 1 picosecond and 1σ being on the order of 1 nanometer. Relaxation curves are shown for a cross-interaction of $\varepsilon_{AB} = 0.5$ is shown below in Figure 2. As predicted, the more a chain alternates between unfavorable monomers, the material exhibits a reduced T_g.

Figure 3 shows the degree of phase separation for both the alternating and decablock chains. The deviation from linearity of the total pair energy in the system is indicative of the system avoiding the unfavorable cross-interactions by settling near similar beads, viz. phase separating. This is especially evident in the supercooled decablock system. While we see T_g suppression as the polymer approaches fully alternating (Figure 4), the atomistic effects of the PS and PEO monomer geometry are lost due to the coarseness in the bead-spring model, and we do not see T_g suppression below that of the strictly alternating chain. We hope to recover this phenomenon in finer-grained simulations in future work.
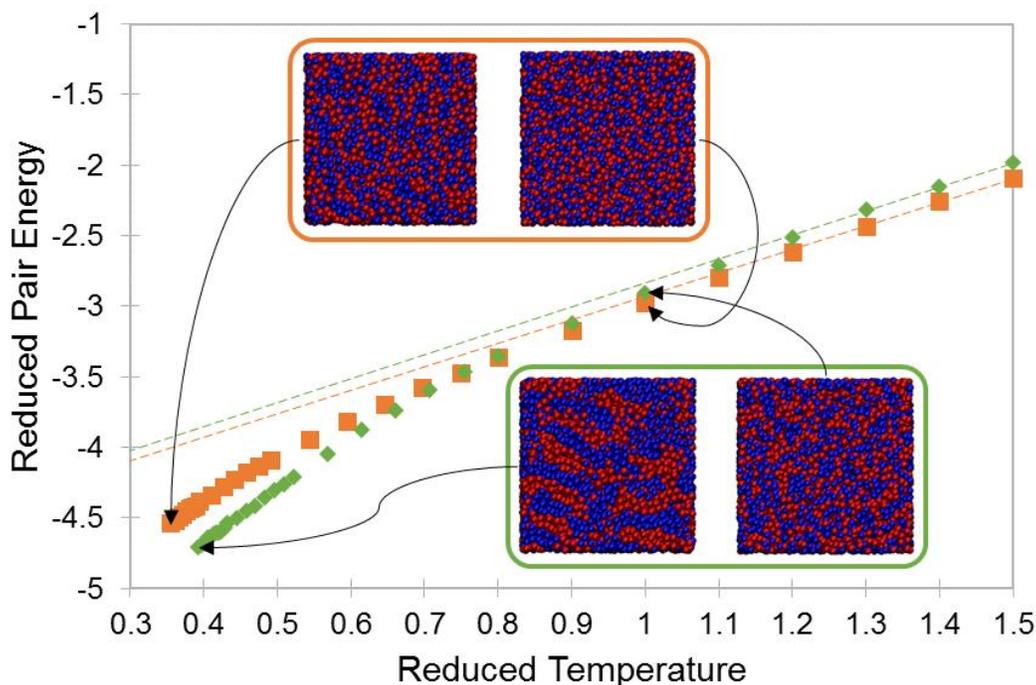

Figure 3. Total pair energies in the bulk for alternating chains (orange squares) and decablock chains (green diamonds). Dashed lines are extended secants from high temperature as a guide-to-the-eye for deviancy from linearity. Inset are high and low temperature cross sections of the bulk equilibrated chains, with arrows point to the corresponding data points.

Computational T_g, or T_g^{comp}, is defined here to be the temperature that exhibits a relaxation time of $\tau_R = 10^4$. These T_g^{comp} values are extrapolated from data shown in Figure 2 and additional sequences with fitting parameters $\{\tau_0, A, T_0\}$ in VFT equation, $\tau_R = \tau_0 \exp\left(\frac{A}{T-T_0}\right)$, and shown against mean block length in Figure 4. Figure 4 suggests two regimes, where the regime for the lower mean block sizes is expected to be affected by sequencing. After crossing some critical mean block size, somewhere in the region of 1.6 on Figure 4, we see a plateau of the $T_g^{comp}/T_g^{comp,pure}$ at approximately 0.925. This plateau seems to align with when the polymer can sufficiently phase separate to minimize the unfavorable cross interaction energies. It is important to note that this regime change shown here appears to be different than that found in thin polymer films[17–19], due to the length scale here (1-10 nm) being an order of magnitude smaller than that found in thin films (10-100 nm).
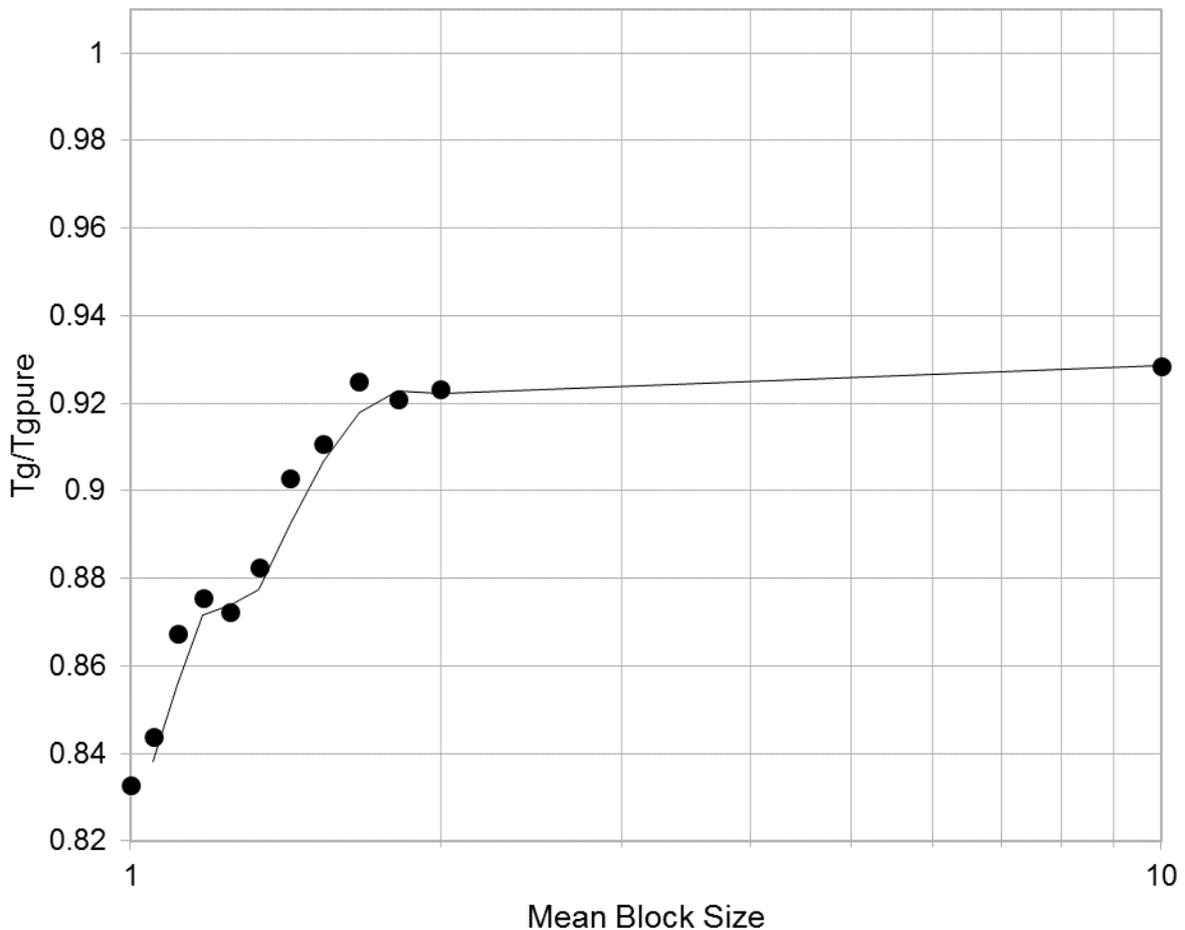
Figure 4. $T_g^{comp}/T_g^{comp,pure}$ plotted against mean block size for random sequences with mean block lengths between that of alternating and decablock chains. In LJ units, $T_g^{comp,pure} = 0.42$. Trendline is a moving average with a period of 2 data points, to show the plateau in the data points.

Lastly, Figure 5 shows relaxation times against inverse temperature. As the cross-interaction energy deviates further from unity, T_g is reduced by an increasing amount for the alternating chain. However, this behavior is not present in the decablock chain, as the larger block sizes allow phase separation. This phase separation lowers the number of contacts between dissimilar monomers, giving a more quantitative analysis of what is shown qualitatively in the Figure 3 insets. This further supports the cross-interaction frustration hypothesis.
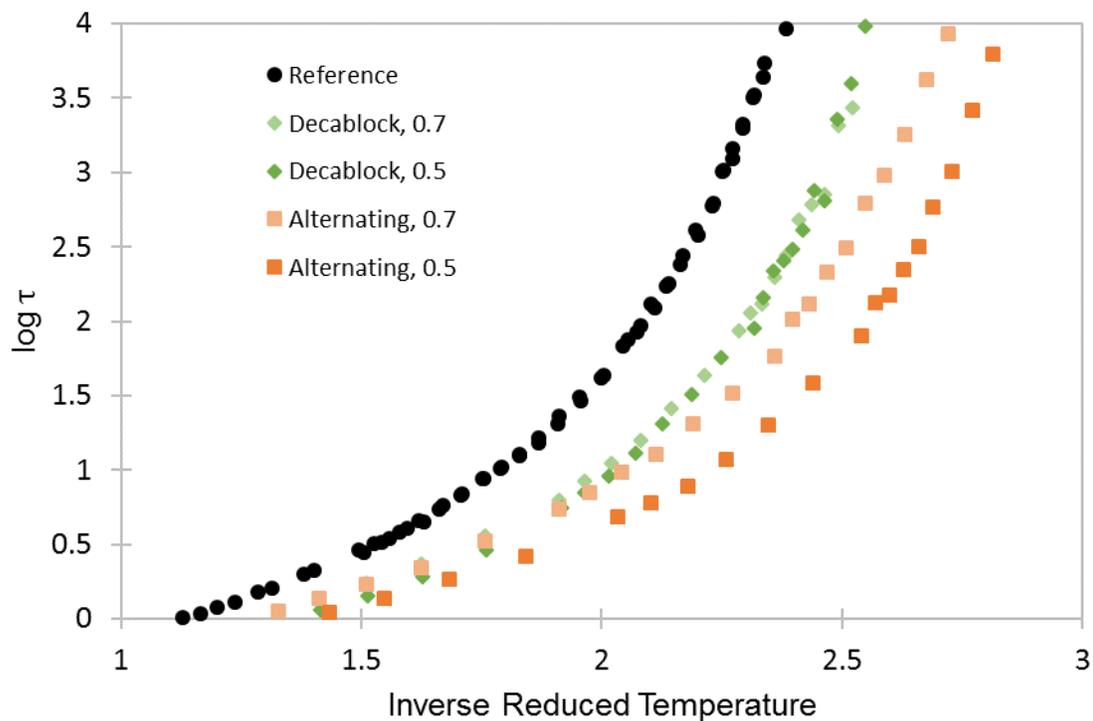
Figure 5. Relaxation curves for alternating and decablock chains with cross-interactions $\varepsilon_{AB} = \{0.5, 0.7\}$. Decreasing the cross-interaction parameter for alternating reduces T_g for the alternating chain, while the decablock chain loses this behavior due to the formation of significantly segregated block domains, as seen in the green inset in Figure 3.

Conclusions

The above work supports the hypothesis of T_g suppression with unfavorable cross interactions the Kremer and Grest model, warranting further sequence-specific study at the bead-spring level, leading to work within a finer-grained, atomistic model that accounts for the geometry and electronic properties of the contrasting monomers. This sequence-specific behavior, transitioning on a length scale of the repeat unit in the polymer chain, is a separate phenomenon than the well-documented T_g apparent in thin polymer films[17–19]. It is expected that in the sequence-controlled regime before the phase-separated plateau shown in Figure 4 that the mean block size itself does not accurately predict the T_g of a specific sequence; in fact, there is likely a distribution of T_g for each mean block size with some sequences suppressing T_g further than others. Due to the coarseness of the bead-spring model and the simplification of the local molecular geometry, this distribution is expected to be broader in a more fine-grained simulation and similarly in the real chain dynamics.

Having shown the sequence dependence of T_g in the bead-spring model, this work lays a foundation for further modelling on a finer-grained, all-atom simulation to test specific monomer pairs and sequences to find ideal polyelectrolyte candidates that avoid crystallization and exhibit cooler liquid behavior, using methodologies such as a neural-networked-biased genetic algorithm[20] to efficiently probe the space of possible polymer sequences for optimal ionic conductivity and thermal behavior. Briefly, this algorithm iterates over possible polymer chains, keeping storage of all previously evaluated samples for reference while using a neural network to suggest new candidates for further improvement in ionic conductivity and T_g suppression. Regardless, the unique physics of the frustrated, low mean block size copolymer system reported here provides opportunities for application of materials beyond that of lithium ion electrolytes, generalizing to any material that requires a beneficial property of one monomer where a detrimental quality of the same monomer can be suppressed by the introduction of a dissimilar monomer.

References

(1)   Kalhoff, J.; Eshetu, G. G.; Bresser, D.; Passerini, S. Safer Electrolytes for Lithium-Ion Batteries: State of the Art and Perspectives. *ChemSusChem* **2015**, *8* (13), 2154–2175.

(2)   Armand, M.; Tarascon, J.-M. Building Better Batteries. *Nature* **2008**, *451* (7179), 652–657.

(3)   Scrosati, B.; Vincent, C. A. Polymer Electrolytes: The Key to Lithium Polymer Batteries. *MRS Bull.* **2000**, *25* (3), 28–30.

(4)   Manuel Stephan, A. Review on Gel Polymer Electrolytes for Lithium Batteries. *Eur. Polym. J.* **2006**, *42* (1), 21–42.

(5)   Jr, T. G. F.; Flory, P. J. Second-Order Transition Temperatures and Related Properties of Polystyrene. I. Influence of Molecular Weight. *J. Appl. Phys.* **1950**, *21* (6), 581–591.

(6)   Tonelli, A. E.; Jhon, Y. K.; Genzer, J. Glass Transition Temperatures of Styrene/4-BrStyrene Copolymers with Variable Co-Monomer Compositions and Sequence Distributions. *Macromolecules* **2010**, *43* (16), 6912–6914.

(7)   Monroe, C.; Newman, J. The Impact of Elastic Deformation on Deposition Kinetics at Lithium/Polymer Interfaces. *J. Electrochem. Soc.* **2005**, *152* (2), A396–A404.

(8)   Kremer, K.; Grest, G. S. Dynamics of Entangled Linear Polymer Melts: A Molecular-dynamics Simulation. *J. Chem. Phys.* **1990**, *92* (8), 5057–5086.

(9)   Vogel, H. Das Temperatur-Abhängigkeitsgesetz Der Viskosität von Flüssigkeiten. *Phys Zeit* **1921**, *22*, 645–646.

(10) Fulcher, G. S. Analysis of Recent Measurements of the Viscosity of Glasses. *J. Am. Ceram. Soc.* **1925**, *8* (6), 339–355.

(11) Tammann, G.; Hesse, W. Die Abhängigkeit Der Viskosität von Der Temperatur Bei Unterkühlten Flüssigkeiten. *Z Anorg Allg Chem* **1926**, *156*, 245–257.

(12) Humphrey, W.; Dalke, A.; Schulten, K. VMD – Visual Molecular Dynamics. *J. Mol. Graph.* **1996**, *14*, 33–38.

(13) Plimpton, S. Fast Parallel Algorithms for Short-Range Molecular Dynamics. *J. Comput. Phys.* **1995**, *117* (1), 1–19.

(14) Grest, G. S.; Kremer, K. Molecular-Dynamics Simulation for Polymers in the Presence of a Heat Bath. *Phys. Rev. A* **1986**, *33* (5), 3628–3631.

(15) Martínez, L.; Andrade, R.; Birgin, E. G.; Martínez, J. M. PACKMOL: A Package for Building Initial Configurations for Molecular Dynamics Simulations. *J. Comput. Chem.* **2009**, *30* (13), 2157–2164.

(16) Hansen, J.-P.; McDonald, I. R. *Theory of Simple Liquids*; Academic Press, 2006.

(17) Roth, C. B.; Dutcher, J. R. Glass Transition and Chain Mobility in Thin Polymer Films. *J. Electroanal. Chem.* **2005**, *584* (1), 13–22.

(18) McKenna, G. B. Ten (or More) Years of Dynamics in Confinement: Perspectives for 2010. *Eur. Phys. J. Spec. Top.* **2010**, *189* (1), 285–302.

(19) Ediger, M. D.; Forrest, J. A. Dynamics near Free Surfaces and the Glass Transition in Thin Polymer Films: A View to the Future. *Macromolecules* **2014**, *47* (2), 471–478.

(20) Patra, T. K.; Meenakshisundaram, V.; Hung, J.-H.; Simmons, D. S. Neural-Network-Biased Genetic Algorithms for Materials Design: Evolutionary Algorithms That Learn. *ACS Comb. Sci.* **2016**.